Chimeric PRMT6 protein produced by an endogenous retrovirus promoter regulates cell fate decision in mouse preimplantation embryos

Shinnosuke Honda, Maho Hatamura, Yuri Kunimoto, Shuntaro Ikeda, and Naojiro Minami

Laboratory of Reproductive Biology, Graduate School of Agriculture, Kyoto University, Kyoto 606-8502, Japan

Corresponding author

Email: minami.naojirou.6r@kyoto-u.ac.jp

https://orcid.org/0000-0002-3191-330

Abstract

Murine endogenous retrovirus with leucine tRNA primer, also known as MERVL, is expressed during zygotic genome activation in mammalian embryos. Here we show that protein arginine N-methyltransferase 6 (*Prmt6*) forms a chimeric transcript with MT2B2, one of the long terminal repeat sequences of MERVL, and is translated into an elongated chimeric protein ($PRMT6^{MT2B2}$) whose function differs from that of the canonical PRMT6 protein ($PRMT6^{CAN}$) in mouse preimplantation embryos. Overexpression of $PRMT6^{CAN}$ in fibroblast cells increased asymmetric dimethylation of the third arginine residue of both histone H2A (H2AR3me2a) and histone H4 (H4R3me2a), while overexpression of $PRMT6^{MT2B2}$ increased only H2AR3me2a. In addition, overexpression of $PRMT6^{MT2B2}$ in one blastomere of mouse two-cell embryos promoted cell proliferation

and differentiation of the blastomere into epiblast cells at the blastocyst stage, while overexpression of PRMT6^{CAN} repressed cell proliferation. This is the first report of the translation of a chimeric protein (PRMT6^{MT2B2}) in mouse preimplantation embryos. Our results suggest that analyzing chimeric transcripts with MERVL will provide insight into the relationship between zygotic genome activation and subsequent intra- and extra-cellular lineage determination. However, more comprehensive proteomic analysis is needed to determine the precise functions of chimeric proteins during preimplantation development.

Key words: Mouse, endogenous retrovirus, *Prmt6*, preimplantation embryo development

Introduction

Immediately after fertilization, mammalian embryos have low transcriptional activity and translate proteins from mRNA stored in oocytes. In mouse embryos, transcription subsequently begins with two waves of zygotic genome activation (ZGA), namely minor and major ZGA, the former during the S phase of the one-cell stage and the latter during the late two-cell stage (Minami et al. 2007; Schulz and Harrison 2019). Before and after major ZGA, the epigenome of the fertilized egg changes dynamically (Burton and Torres-Padilla 2010; Xu et al. 2021). Epigenetic modifications, including DNA methylation and histone modifications, are known to be important for cell differentiation during development (Wu and Yi 2006). For example, *Carm1*, encoding a protein arginine methyltransferase, has been reported to be involved in the differentiation of blastomeres into epiblast cells through the dimethylation of histone arginine residues in mouse preimplantation embryos (Torres-Padilla et al. 2007; White et al. 2016). Endogenous retroviruses (ERVs) are one of the components of transposable elements and

occupy about 10% of human and mouse genomes (Waterston et al. 2002; Ito et al. 2020). Although ERVs are among the earliest transcribed genetic material in mouse preimplantation embryos (Kigami et al. 2003) and various studies have shown that ERVs are expressed in mammalian preimplantation embryos (Wang et al. 2001; Poznanski and Calarco 1991; Evsikov et al. 2004), there is little direct evidence that ERVs regulate cell differentiation. The high abundance of ERVs in the mammalian genome (Ito et al. 2020) and the fact that several ERV-derived genes, such as *Syncytin* and *Peg10*, are essential for placentation (Sha et al. 2000; Dupressoir et al. 2009, 2012; Suzuki et al. 2007) suggest that ERVs were involved in the evolution of the placenta in mammals. Murine or human endogenous retrovirus with leucine tRNA primer (MERVL or HERVL, respectively) is a transposable element expressed during major ZGA in mice and humans (Macfarlan et al. 2012; Wang et al. 2001; Kigami et al. 2003; Franke et al. 2017). It has been reported that MERVL-activated mouse embryonic stem cells injected into eight-cell embryos can also contribute to extra-embryonic tissues (Yang et al. 2020), suggesting that some MERVL/HERVL elements may regulate the totipotency of mammalian embryos. Recently, a MERVL-derived non-coding RNA called LincGET was shown to control the differentiation of embryonic and extra-embryonic tissues in mouse preimplantation embryos (Wang et al. 2018), but the function of the vast majority of MERVL elements remains to be elucidated. Several studies have shown that the long terminal repeat of MERVL generates chimeric transcripts with host genes during early embryonic development (Peaston et al. 2004; Macfarlan et al. 2012). Because MERVL has been reported to be one of the earliest transcribed genomic sequences in preimplantation embryos (Kigami et al. 2003; Wang et al. 2001), we hypothesized that MERVL chimeric transcripts contribute to the cell lineage differentiation that occurs after major ZGA

(Chazaud and Yamanaka 2016).

Reanalysis of previously reported RNA-sequencing (RNA-seq) data revealed that protein arginine N-methyltransferase 6 (*Prmt6*) expression is activated by the MERVL promoter sequence in preimplantation embryos. Like *Carm1*, *Prmt6* encodes a Type-I protein arginine methyltransferase (Di Lorenzo and Bedford 2011) and has been shown to regulate the epigenome by the asymmetric di-methylation of arginine residues in histone proteins (Guccione et al. 2007; Hyllus et al. 2007; Kirmizis et al. 2007). Furthermore, overexpression or suppression of *Prmt6* in embryonic stem cells results in the loss of pluripotency and in the increased expression of differentiation marker genes (Lee et al. 2012). In the course of analyzing transcripts involved in MERVL in mouse preimplantation embryos, it was discovered that *Prmt6* has two transcripts of different lengths. One is the canonical *Prmt6* transcript ($Prmt6^{CAN}$), and the other is $Prmt6^{MT2B2}$, defined as the chimeric transcript of $Prmt6^{CAN}$ with MT2B2, the MERVL long terminal repeat sequence. It was also found that the chimeric transcript produced an elongated PRMT6 chimeric protein ($PRMT6^{MT2B2}$). In addition, the chimeric protein has different histone modification specificity from that of the canonical PRMT6 protein ($PRMT6^{CAN}$), and overexpression of the chimeric protein in one blastomere of two-cell embryos promotes its contribution to the embryonic cell lineage. These findings shed light on a new aspect of the differentiation mechanism during embryogenesis.

Results

Screening of candidate MERVL chimeric transcripts associated with cell lineage differentiation

Macfarlan et al. published a list of MERVL chimeric transcripts in mouse two-

cell stage embryos (Macfarlan et al. 2012), and we compared these transcripts with histone modification–related genes (Fig. 1A). Eight genes (*Atxn7*, *Brms1l*, *Ctcf*, *Kdm4c*, *Pcgf5*, *Prmt6*, *Rnf20*, and *Smyd3*) overlapped, and half of them (*Ctcf*, *Kdm4c*, *Rnf20*, and *Smyd3*) had already been reported to be important in early embryonic development (Wang et al. 2010; Suzuki et al. 2015; Ooga et al. 2015; Wan et al. 2008). Analysis of a published RNA-seq dataset (Zhang et al. 2016) revealed that the expression levels of four of the eight genes (*Ctcf*, *Kdm4c*, *Pcgf5*, and *Prmt6*) were more than twice as high in late two-cell embryos compared with early two-cell embryos (Fig. 1B)

Expression dynamics of chimeric and canonical Prmt6 mRNA in mouse preimplantation embryos

Genomic analysis in mice revealed that MT2B2 is located 212 bp upstream of the first exon of *Prmt6*, and that the chimeric transcript is transcribed from this position. To determine the expression profiles of $Prmt6^{MT2B2}$ and $Prmt6^{CAN}$, the amounts of total *Prmt6* transcripts ($Prmt6^{MT2B2}$ and $Prmt6^{CAN}$) and $Prmt6^{MT2B2}$ during preimplantation development were determined by quantitative RT-PCR (Fig. 2A). As expected, the amounts of total *Prmt6* transcripts and $Prmt6^{MT2B2}$ transcripts in the late two-cell stage were increased at major ZGA and gradually decreased by the blastocyst stage (Fig. 2B). At the blastocyst stage, $Prmt6^{MT2B2}$ transcripts had almost completely disappeared, but $Prmt6^{CAN}$ transcripts were still present, albeit in small amounts (Fig. 2B). To compare the exact copy numbers of each transcript, absolute quantification was performed using late two-cell embryos and blastocysts. In late two-cell embryos, the amounts of total *Prmt6* transcripts and chimeric transcripts were almost the same (Fig. 2C). In blastocysts, on the other hand, the copy number of $Prmt6^{MT2B2}$ transcripts was significantly lower than that

of total *Prmt6* transcripts (Fig. 2C). Furthermore, microinjecting zygotes with si*Prmt6*^{MT2B2} (siRNA targeting the sequence between the MT2B2 and *Prmt6*^{CAN} transcription start sites) or si*Prmt6*^{CAN}-1 or si*Prmt6*^{CAN}-2 (siRNAs targeting the *Prmt6* exon sequence, see Fig. 2A) resulted in a significant decrease in transcript levels of both total *Prmt6* transcripts and *Prmt6*^{MT2B2} transcripts at the late two-cell stage (Fig. 2D). Since trimethylation of the fourth lysine residue of histone H3 (H3K4me3) is generally increased around transcription start sites, we analyzed the previously reported chromatin immunoprecipitation sequencing (ChIP-seq) data of H3K4me3 (Liu et al. 2016) in preimplantation embryos and found that the H3K4me3 ChIP-seq peak shifted from the MT2B2 region to just before the first exon of *Prmt6*^{CAN} as development progressed from the four-cell stage to the blastocyst stage (Fig. 2E).

Identification of the translation initiation codon of the PRMT6^{MT2B2} *chimeric protein*

Since *Prmt6*^{MT2B2} has an extended sequence on the 5' side of *Prmt6*^{CAN} and two putative translation initiation codons exist in this region, we sought to determine the site where translation of the chimeric transcript began (Fig. 3A). Western blotting of the PRMT6 protein using metaphase II (MII) oocytes and fertilized eggs at each developmental stage revealed that ~55 kDa bands were detected in oocytes and embryos during all developmental stages, and an additional ~42 kDa band was detected only in embryos at the blastocyst stage (Fig. 3B). Since PRMT6^{CAN} has a molecular weight of ~42 kDa, mRNAs of *Prmt6*^{CAN} and *Prmt6*^{MT2B2} were generated by in vitro transcription to identify the translation product of the ~55 kDa protein detected at each developmental stage. The mRNAs transfected into NIH3T3 cells revealed that *Prmt6*^{MT2B2} mRNA encodes an elongated protein of ~55 kDa, while *Prmt6*^{CAN} mRNA encodes a protein of

~42 kDa (Fig. 3C). Consistent with the amount of transcript, PRMT6^{MT2B2} with a molecular weight of ~55 kDa was most abundant at the late two-cell stage and gradually decreased until the blastocyst stage (Fig. 3B). There are two candidate translation initiation codons (Met1 and Met2) for *Prmt6*^{MT2B2}, and Met3 is the translation initiation codon for PRMT6^{CAN} (Fig. 3A). To determine which codon *Prmt6*^{MT2B2} is translated from, three types of mRNAs mutated in Met1, Met2, or Met3 (AUG to AAG) were transfected into NIH3T3 cells. Among NIH3T3 cells transfected with the three mutant mRNAs, only those with the Met1 mutant transcript failed to produce the ~55 kDa PRMT6^{MT2B2} (Fig. 3C). The same results were obtained using mouse four-cell embryos (Fig. 3C). Bands at ~55 kDa were detected in all four-cell embryos because these embryos express the endogenous PRMT6^{MT2B2} (Fig. 3C). Knockdown of endogenous *Prmt6* transcripts with siRNAs (si*Prmt6*^{CAN}-1 or si*Prmt6*^{CMT2B2}) at the one-cell stage decreased the amount of the ~55 kDa protein at the four-cell stage (Fig. 3D).

Functional analysis of the PRMT6^{MT2B2} *chimeric protein*

Three-dimensional structure prediction using AlphaFold (Jumper et al. 2021) showed no structural change in the S-adenosylmethionine–dependent methyltransferase domain of PRMT6^{MT2B2} compared to PRMT6^{CAN} (Fig. 4A). Therefore, the ~55 kDa PRMT6^{MT2B2} was considered to have arginine methylation activity, and the function of this protein and its involvement in cell differentiation in mammalian preimplantation embryos were examined. Since PRMT6^{CAN} is known to be a type I protein arginine methyltransferase (Di Lorenzo and Bedford 2011), western blotting was performed using various histone arginine asymmetric dimethylation antibodies to confirm the histone arginine methylation status of NIH3T3 cells overexpressing PRMT6^{CAN} or PRMT6^{MT2B2}.

Overexpression of PRMT6^{CAN} significantly increased asymmetric dimethylation of the third arginine residue of both histone H2A (H2AR3me2a) and histone H4 (H4R3me2a) (Fig. 4B, 4C, 4D). By contrast, overexpression of PRMT6^{MT2B2} significantly increased asymmetric dimethylation of only H2AR3me2a (Fig. 4B, 4C, 4D; $P<0.01$).

PRMT6^{MT2B2} regulates cell differentiation in mouse preimplantation embryos

Prmt6^{CAN} or *Prmt6^{MT2B2}* mRNA together with *H2B-EGFP* mRNA as a lineage tracer was microinjected into one blastomere of two-cell embryos to examine the effects on cell lineage specification in mouse preimplantation embryos (Fig. 5A). Overexpression of PRMT6^{CAN} significantly reduced the number of H2B-EGFP–positive cells in blastocysts at 96 h post insemination (hpi) compared to H2B-EGFP–negative cells, while PRMT6^{MT2B2} overexpression increased the number of H2B-EGFP–positive cells in blastocysts at 96 hpi (Fig. 5B, 5C). Overexpression of H2B-EGFP alone did not affect the number of H2B-EGFP–positive cells in blastocysts. In addition, overexpression of PRMT6^{MT2B2} significantly increased the number of cells that differentiated into NANOG-positive epiblast cells in blastocysts (Fig. 5B, 5D), while this number was unaffected by H2B-EGFP alone or PRMT6^{CAN} overexpression (Fig. 5D).

Discussion

Among the histone modification–related genes expressed as chimeric transcripts with MERVL, the expression of four genes (*Ctcf, Kdm4c, Pcgf5,* and *Prmt6*) dramatically increased during major ZGA, suggesting that many genes expressed during this period may be mainly under control of the MERVL promoter. Indeed, the results of absolute quantitative RT-PCR (Fig. 2C) and siRNA knockdown experiments targeting the

intermediate sequence between MT2B2 and *Prmt6* exon (Fig. 2D) showed that almost all *Prmt6* transcripts were *Prmt6*^{MT2B2} at the late two-cell stage. In contrast, most *Prmt6*^{CAN} transcripts were expressed at the blastocyst stage, indicating that the transcriptional machinery of *Prmt6* is dramatically altered during early embryogenesis.

Overexpression experiments of *Prmt6*^{MT2B2} mRNA with a mutation in the translation initiation codon revealed that the *Prmt6*^{MT2B2} chimeric transcript is translated into the PRMT6^{MT2B2} chimeric protein from the 5'-extended uppermost ATG codon (Fig. 3C, 3D). PRMT6^{MT2B2} is the first MERVL chimeric protein translated from a chimeric transcript during mammalian development. Outside of early embryogenesis, one case of a MERVL chimeric transcript translated into a longer protein was reported in cancer cells (Lock et al. 2014). Since the extended 56-amino-acid sequence of PRMT6^{MT2B2} showed no homology to retrovirus-derived proteins such as the GAG protein (data not shown), further studies on the origin of the elongated sequence are needed to understand the biological functions of PRMT6^{MT2B2} chimeric proteins. Although many chimeric transcripts are expressed in cancer cells and embryonic stem cells (Babaian and Mager 2016; Macfarlan et al. 2012), their exact translation initiation codons and biological functions remain unknown, and more comprehensive proteomic analysis is needed to understand the precise function of chimeric transcripts, including those expressed in preimplantation embryos.

Our results also revealed that the PRMT6^{MT2B2} chimeric protein has more substrate-specific histone arginine methylation activity than PRMT6^{CAN} (Fig. 4B, 4C), suggesting that changes in epigenomic modifications may regulate developmental progression and gene expression in early preimplantation embryos. PRMT6 is known to be expressed in several cancer tissues, including colorectal, breast, bladder, and lung

adenocarcinomas (Avasarala et al. 2020; Lim et al. 2018; Yoshimatsu et al. 2011; Tang et al. 2020; Veland et al. 2017). Investigating how PRMT6^{MT2B2} is associated with cancer progression will provide insight into the involvement of retroviruses in cancer development (Gonzalez-Cao et al. 2016; Attermann et al. 2018; Kassiotis and Stoye 2016; Babaian and Mager 2016) and a new perspective on cancer research. The PRMT6^{CAN} protein contains a nuclear localization signal (NLS) at the N-terminus (Fig. 3A) (Herrmann et al. 2005; Frankel et al. 2002). Since it is known that the modification of surrounding amino acids and protein conformation affect NLS function (Sorokin et al. 2007), it is possible that the NLS does not function properly due to the extended amino acid sequence of PRMT6^{MT2B2}. Since other arginine methyltransferases are known to methylate proteins localized in the cytoplasm (Litt et al. 2009; Di Lorenzo and Bedford 2011), analysis of the subcellular localization of PRMT6^{MT2B2} could provide new insights into its function.

In blastocysts, most *Prmt6* transcripts are presumably *Prmt6^{CAN}* based on absolute quantification (Fig. 2C). Blastomeres overexpressing PRMT6^{MT2B2} were more likely to consist of epiblast cells than non-injected blastomeres, while those overexpressing PRMT6^{CAN} did not contribute to each cell lineage (Fig. 4G). This indicates that PRMT6^{MT2B2} and PRMT6^{CAN} have different functions in cell differentiation during embryogenesis. It has been reported that H3R2me2a mediated by PRMT6^{CAN} recruits Aurora B to chromosome arms (Kim et al. 2020) and that overexpression of Aurora B facilitates cell contribution to the placental cell lineage by regulating the nuclear dynamics of OCT4 in mouse preimplantation embryos (Li et al. 2017; Plachta et al. 2011). Based on these results, it is conceivable that an increased ratio of PRMT6^{CAN} to PRMT6^{MT2B2} promotes cell differentiation during the blastocyst

stage through localization of PRMT6^{CAN} in the nucleus. In addition, several protein arginine methyltransferases have been reported to act redundantly (Cheng et al. 2020; Wei et al. 2021). *Carm1* was found to promote differentiation of blastomeres to epiblast cells via methylation of H3R26me2 (Torres-Padilla et al. 2007; White et al. 2016; Goolam et al. 2016), and *Prmt1* enzymic inhibitor promoted the differentiation of embryonic stem cells into primitive endoderm via Klf4 methylation (Zuo et al. 2022). These results support the possibility that PRMT6^{MT2B2}, but not PRMT6^{CAN}, may regulate the differentiation pathways in blastocysts. Since recent studies have shown that gene expression heterogeneity and blastomere differentiation begin in the late two-cell stage in mouse embryos (Wang et al. 2018; Jin et al. 2022; Wang et al. 2021; Krawczyk et al. 2021), it is possible that PRMT6^{MT2B2} is also involved in heterogeneous gene expression in blastomeres during this stage, thereby regulating cell differentiation in early development.

Overexpression of PRMT6^{CAN} in a single blastomere in two-cell stage embryos resulted in delayed cell proliferation (Fig. 4F), probably since PRMT6^{CAN} disrupts the cell cycle, as reported in previous studies (Kim et al. 2020; Schneider et al. 2021). On the other hand, overexpression of PRMT6^{MT2B2} promoted cell proliferation (Fig. 4F), indicating that PRMT6^{CAN} and PRMT6^{MT2B2} affect cell proliferation in opposite ways. Modzelewski et al. reported that the MERVL-*Cdk2ap1* chimeric transcript is translated into a shorter protein (CDK2AP1$^{\Delta N}$) than the canonical protein (CDK1AP1^{CAN}) in early mammalian embryos, and that CDK2AP1$^{\Delta N}$ promotes cell proliferation while CDK2AP1^{CAN} inhibits the cell cycle (Modzelewski et al. 2021). These findings and our own indicate that chimeric transcripts expressed during major ZGA mediate different functions than canonical transcripts.

In conclusion, we have shown that the chimeric transcript *Prmt6*^{MT2B2} is expressed in mouse preimplantation embryos and that it generates the chimeric protein PRMT6^{MT2B2} during major ZGA. Furthermore, PRMT6^{MT2B2} expressed in early preimplantation embryos is involved in determining cell differentiation during the blastocyst stage. This study reveals that MERVL expressed at major ZGA regulates cell differentiation during embryogenesis by regulating the expression of nearby genes and the translation of their corresponding mRNA.

Materials and Methods

In vitro fertilization and embryo culture

Eight- to twelve-week-old ICR female mice (Japan SLC, Hamamatsu, Japan) were superovulated by injection of 5 IU of equine chorionic gonadotropin (eCG; ASKA Pharmaceutical, Tokyo, Japan) followed by 5 IU of human chorionic gonadotropin (hCG; ASKA Pharmaceutical) 48 h later. Cumulus oocyte complexes were harvested 14 h after hCG injection and placed in human tubal fluid (HTF) medium supplemented with 4 mg/ml bovine serum albumin (BSA, A3311; Sigma-Aldrich, St. Louis, MO) covered with paraffin oil (Nacalai Tesque, Kyoto, Japan). Spermatozoa were collected from the cauda epididymis of 13–20-week-old ICR male mice (Japan SLC) and cultured in HTF medium for 1 h. After capacitation, sperm were introduced into oocyte-containing droplets at a final concentration of 1×10^6 cells/ml. After 3-h incubation at 37°C in an atmosphere of 5% CO_2, fertilized oocytes were washed with K^+-modified simplex optimized medium (KSOM) supplemented with amino acids (Ho et al. 1995) and 1 mg/ml BSA, and then used for microinjection or cultured in the same medium under paraffin oil at 37°C in an atmosphere of 5% CO_2 to the following stages: one-cell (12 h post insemination (hpi)), early two-cell (24 hpi), late two-cell (36 hpi), four-cell (48 hpi), eight-cell (54 hpi), morula (72 hpi), and blastocyst (96 hpi). MII oocytes were collected from cumulus oocyte complexes followed by treatment with 1% hyaluronidase to remove cumulus cells.

Plasmid construction, in vitro transcription, and microinjection

Based on the transcription start site of *Prmt6*^{CAN} predicted from the NCBI database (NM_178891.5) and that of *Prmt6*^{MT2B2} predicted from previously reported RNA-seq data (Liu et al. 2016), the sequences of *Prmt6*^{CAN} and *Prmt6*^{MT2B2} were cloned

by PCR from the cDNA of late two-cell embryos. The amplified products were digested with EcoRI and XbaI, and the fragments were incorporated into a pBluescript II SK (−) vector plasmid (Agilent Technologies Japan, Hachioji, Japan). Start codon mutant constructs were generated by mutation PCR using the PrimeSTAR Mutagenesis Basal Kit (Takara Bio, Kusatsu, Japan) by replacing AUG with AAG at Met1, Met2, or Met3. The AAG codon was chosen because this mutation has been reported to cause complete loss of translational activity in eukaryotic cells compared to other single-nucleotide mutations (Wei et al. 2013). Methylase-inactive KLA mutant constructs were generated using the same method by replacing amino acids Val–Leu–Asp at positions 89–91 in $PRMT6^{CAN}$ with Lys–Leu–Ala to produce $PRMT^{CAN}$-KLA (Boulanger et al. 2005), or by replacing these amino acids at positions 145–147 in $PRMT6^{MT2B2}$ with Lys–Leu–Ala to produce $PRMT6^{MT2B2}$-KLA. Each mRNA was synthesized with the mMESSAGE mMECHINE T7 Ultra Kit (Thermo Fisher Scientific, Waltham, MA), purified with the RNeasy Mini Kit (Qiagen, Hilden, Germany), and then dissolved in nuclease-free water. For knockdown experiments, siRNAs (RNAi, Tokyo, Japan) dissolved in nuclease-free water at a concentration of 100 μM were used for microinjection. For overexpression experiments, $Prmt6^{CAN}$ or $Prmt6^{MT2B2}$ mRNA was diluted to 250 ng/μl and co-injected with *H2B-EGFP* mRNA at a concentration of 100 ng/μl. Approximately 5–10 pl of mRNA or siRNA was microinjected into the cytoplasm of one-cell embryos at 3–5 hpi or into the cytoplasm of one blastomere of two-cell embryos at 24–26 hpi in HEPES-buffered KSOM. Microinjection was performed under an inverted microscope (IX73; Olympus, Tokyo, Japan) equipped with a piezo injector (PMAS-CT150; PRIME TECH, Tokyo, Japan) and a micromanipulator (IM-11-2; Narishige, Tokyo, Japan). The primers and siRNA sequences are listed in Supplementary Tables 1 and 2.

Cell culture and mRNA transfection

NIH/3T3 cells were cultured in Dulbecco's modified Eagle's medium supplemented with 10% calf serum, 75 µg/ml penicillin, and 50 µg/ml streptomycin. mRNAs transcribed in vitro were transfected into 50–60% confluent cells using Lipofectamine MessengerMAX Transfection Reagent (Thermo Fisher Scientific). Twenty-four hours after transfection, the cells were washed in phosphate-buffered saline (PBS) once and then lysed in 1X Laemmli sample buffer.

RNA extraction and quantitative RT-PCR

RNA extraction and reverse transcription were performed using the SuperPrep II Cell Lysis & RT Kit for qPCR (Toyobo, Osaka, Japan). Briefly, five embryos or oocytes were washed three times in PBS containing 0.5% polyvinylpyrrolidone (PVP K-30; Nacalai Tesque) (PVP-PBS) and collected in PCR tubes along with 0.5 µl of PVP-PBS. After adding 3.5 µl of lysate, all lysates were subjected to reverse transcription. Transcription levels were measured using the StepOnePlus real-time PCR system (Thermo Fisher Scientific) with KOD SYBR qPCR Mix (Toyobo), and relative gene expression was calculated using the $2^{-\Delta\Delta Ct}$ method normalized against the corresponding *H2afz* levels (Livak and Schmittgen 2001; Jeong et al. 2014). Absolute expression was determined using serial dilutions of the chimeric *Prmt6* cloned plasmid for in vitro transcription or using the pTAC plasmid in which an H2afz PCR fragment was cloned. The primers used for quantification are listed in Supplementary Table 2.

Western blotting

Fifty embryos or oocytes, excluding blastocysts, were washed three times in PVP-PBS and collected in 1X Laemmli sample buffer. Twenty-five blastocysts were collected. After boiling at 95°C for 5 min, the samples were kept at −80°C until use. NIH3T3 cells were directly lysed in 1X Laemmli sample buffer. To analyze histone arginine methylation modifications in NIH3T3 cells, TagRFP, PRMT6^{CAN}-KLA, or PRMT6^{MT2B2}-KLA were used as negative controls for overexpression. Total protein was separated by SDS–polyacrylamide gel electrophoresis (SDS-PAGE) and transferred into a 0.22-μm-pore polyvinylidene fluoride (PVDF) membrane (Cytiva, Tokyo, Japan). After one wash in PBS containing 0.1% Tween (PBST), the membrane was blocked in PBST containing 5% BSA for 1 h at room temperature, followed by incubation with a rabbit anti-PRMT6 antibody (1:1500 dilution; 15395-1-AP; Proteintech, Rosemont, IL), a rabbit anti-H2AR3me2a antibody (1:1000 dilution; ab21574; Abcam, Cambridge, UK), a rabbit anti-H4R3me2a antibody (1:500 dilution; 39706; Active Motif, Carlsbad, CA), a rabbit anti-H3R2me2a antibody (1:1000 dilution; ab175007; Abcam), a rabbit anti-H3R8me2a antibody (1:500 dilution; 39652; Active Motif), a rabbit anti-H3R17me2a antibody (1:2000 dilution; 39710; Active Motif), a rabbit anti-H3R26me2 antibody (1:8000 dilution; 07-215; Merck, Darmstadt, Germany), a mouse anti–β-actin antibody (1:5000 dilution; A5441; Merck), or a rabbit anti–whole-H3 antibody (1:1000 dilution; #9715; Cell Signaling, Danvers, MA) in PBST containing 1% BSA overnight at 4°C. After three washes in PBST, the membrane was incubated with a horseradish peroxidase–conjugated anti-mouse secondary antibody (1:10000 dilution; NA931; Cytiva) or anti-rabbit secondary antibody (1:10000 dilution; NA934; Cytiva) in PBST containing 1% BSA for 1 h at room temperature. After three washes in PBST, the membrane was developed using ImmunoStar LD (FUJIFILM Wako Pure Chemical Corporation, Osaka, Japan) and

scanned with c-DiGit (LI-COR, Lincoln, NE). Densitometric quantification of the immunoblot bands was performed using Image Studio software (LI-COR).

Immunofluorescence

Embryos were fixed in PBS containing 4% paraformaldehyde for 20 min at 28°C. After three washes in PVP-PBS, embryos were permeabilized with 0.5% Triton X-100 (Sigma-Aldrich) in PBS for 40 min at 28°C. After washing three times in PVP-PBS, embryos were blocked in PBS containing 1.5% BSA, 0.02% Tween 20, and 0.2% sodium azide (blocking buffer) for 1 h at 28°C, and then incubated overnight at 4°C with a rabbit anti-NANOG antibody (1:100 dilution; RCAB002P-F; ReproCELL, Kanagawa, Japan) and a mouse anti-CDX2 antibody (1:100 dilution; MU392A-UC; Biogenex, Fremont, CA). After three washes in blocking buffer, embryos were incubated in blocking buffer containing secondary antibodies (Alexa Fluor 555 donkey anti-rabbit IgG, 1:500 dilution, A31572, Thermo Fisher Scientific; Alexa Fluor 647 donkey anti-mouse IgG, 1:500 dilution, A31571, Thermo Fisher Scientific) for 1 h at 28°C. After washing three times in blocking buffer, nuclei were stained in blocking buffer containing 10 μg/ml Hoechst 33342 (Sigma-Aldrich) for 10 min at 28°C. Stained embryos were mounted on slide glass in blocking buffer containing 50% glycerol and signals were observed with a confocal fluorescent microscope (LSM880; Zeiss, Oberkochen, Germany). H2B-EGFP protein was detected based on its own fluorescence.

RNA-seq and ChIP-seq data processing

The bulk RNA-seq data (GSE71434) of embryos of each stage were downloaded and then mapped to the mm10 with STAR (v. 2.7.10a) (Dobin et al. 2013). The gene

expression level was estimated using RSEM (v. 1.3.3) (Li and Dewey 2011) and normalized with the transcripts per kilobase million method. The H3K4me3 ChIP-seq data of mouse preimplantation embryos were downloaded from GSE73952 and mapped to the mm10 with bowtie2 (v. 2.4.5) (Langmead and Salzberg 2012). In all cases, Bam files of biological replicates were merged using samtools (v. 1.10) (Li et al. 2009), normalized by counts per million using deeptools (v. 3.5.1) (Ramírez et al. 2016), and visualized using Integrative Genomics Viewer software (v. 2.12.1) (Robinson et al. 2011).

Three-dimensional Structure Prediction of the PRMT6^{MT2B2} Protein

PRMT6^{CAN} and PRMT6^{MT2B2} protein structure prediction was performed using Alphafold (Jumper et al. 2021) on the Google Colaboratory site (https://colab.research.google.com/github/sokrypton/ColabFold/blob/main/AlphaFold2.ipynb). Obtained data were visualized using the Mol* site (Sehnal et al. 2021) (https://molstar.org/).

Statistical analyses

Each experiment was repeated at least three times. Quantitative RT-PCR data were analyzed by Student's t-test for pairwise comparisons or by Dunnett's test for multiple comparisons. Quantification of western blotting was performed using the Tukey-Kramer test. Cell contribution assays were analyzed with the Wilcoxon signed-rank test. All analyses were performed using R (v. 4.2.1), and significance was accepted at P-values < 0.05.

Ethical approval for the use of animals

All animal experiments were approved by the Animal Research Committee of Kyoto University (Permit Numbers: R3-17) and were performed in accordance with the committee's guidelines.

Acknowledgments

Confocal fluorescent microscopy was performed at the iCeMS Analysis Center, Institute for Integrated Cell-Material Sciences (iCeMS), Kyoto University Institute for Advanced Study (KUIAS). This work was supported by a Grant-in-Aid for Scientific Research (no. 19H03136 to N.M.) and a Grant-in-Aid for JSPS Fellows (no. 19J23290 to S.H.) from the Japan Society for the Promotion of Science.

A

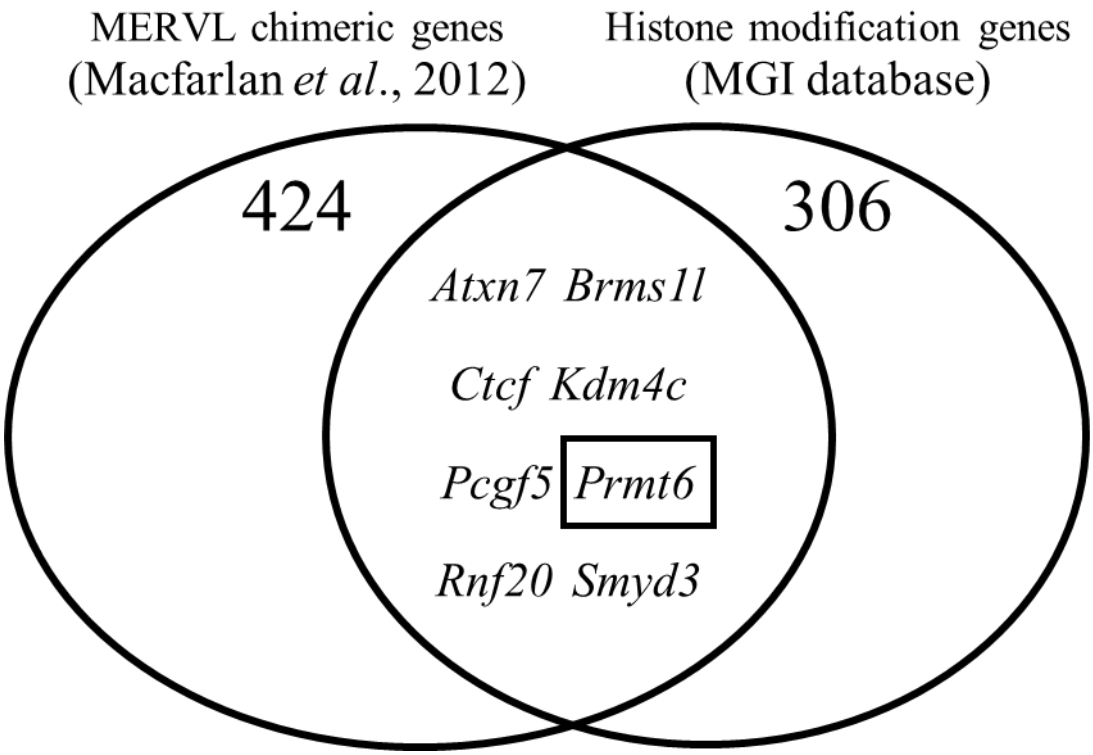

Fig. 1. Verification of MERVL-mediated chimeric genes.

(A) Venn diagram showing overlap of genes expressed as chimeric transcripts with MERVL- and histone modification–related genes.

B

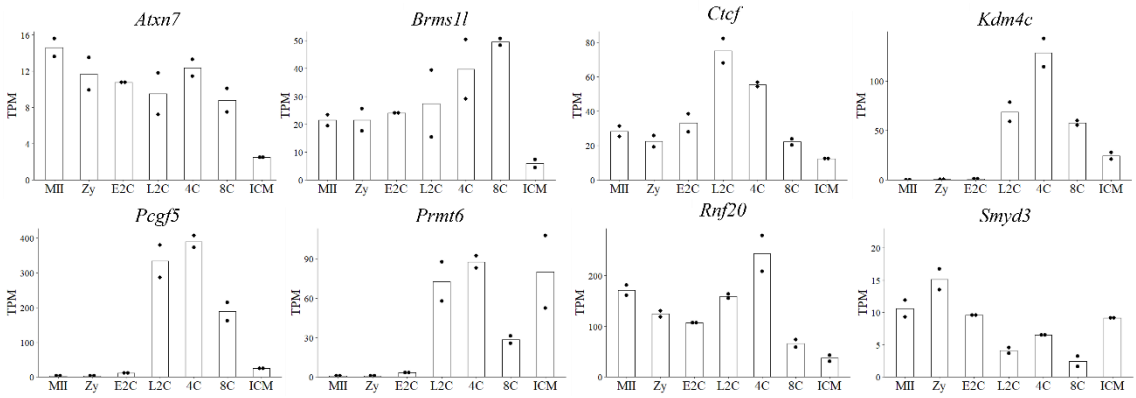

(B) The expression patterns of eight overlapping genes in MII oocytes and preimplantation embryos. Dots represent replicates. Data were obtained from GSE71434. MII: MII oocytes, Zy: zygotes, E2C: early two-cell embryos, 4C: four-cell embryos, 8C: eight-cell embryos, ICM: inner cell mass cells.

A

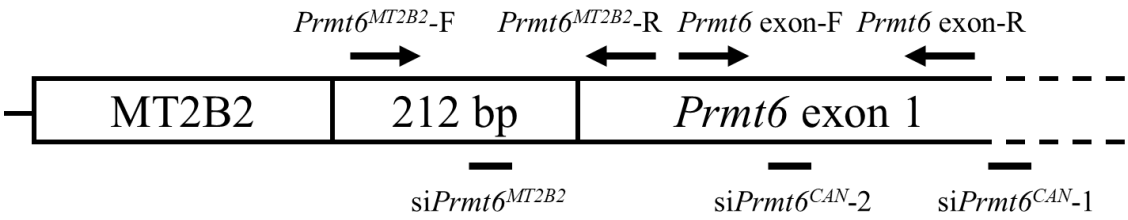

Fig. 2. Gene structure and transcriptional profile of *Prmt6* in mice.

(A) Schematic diagram showing the positions of MT2B2 and *Prmt6* in the mouse genome. MT2B2 is located 212 bp upstream from the transcription start site of *Prmt6*. The names of primers and targeting loci (arrows) are indicated above the diagram, and the names of siRNAs and their targeting sites (bars) are indicated underneath.

B

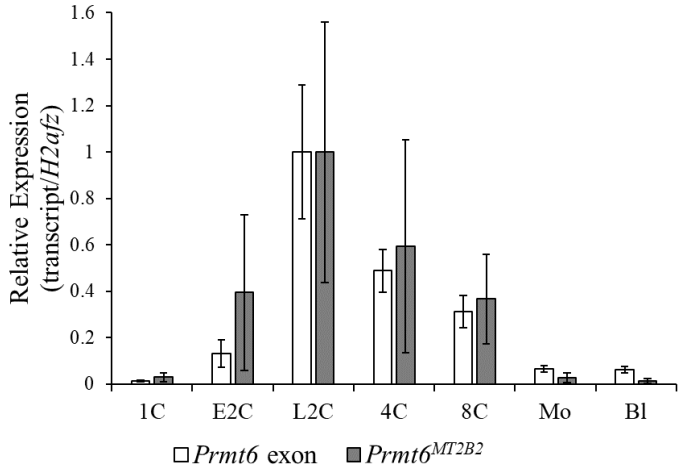

(B) qRT-PCR analysis of the *Prmt6* exon and *Prmt6*^{MT2B2} transcripts during mouse preimplantation development. The amount of mRNA in one-cell embryos was defined as 1, and the expression levels were normalized to *H2afz* as an internal control. Data are expressed as mean ± s.e.m. (n=3).

1C: one-cell embryo, E2C: early two-cell embryo, L2C: late two-cell embryo, 4C: four-cell embryo, 8C: eight-cell embryo, Mo: morula, Bl: blastocyst

C

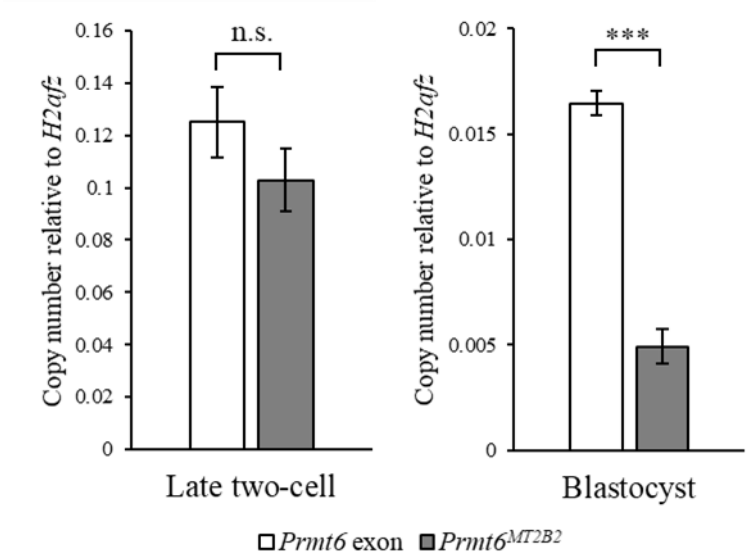

(C) Comparison of expression levels of the *Prmt6* exon and *Prmt6*^{MT2B2} in late two-cell embryos and blastocysts based on absolute quantification by qRT-PCR. Each graph shows the expression levels of each transcript in late two-cell embryos and blastocysts. Copy numbers were normalized to *H2afz* copy numbers. Data are expressed as mean ± s.e.m. (n=5). Student's t-test, ***P < 0.001; n.s., not significant.

D

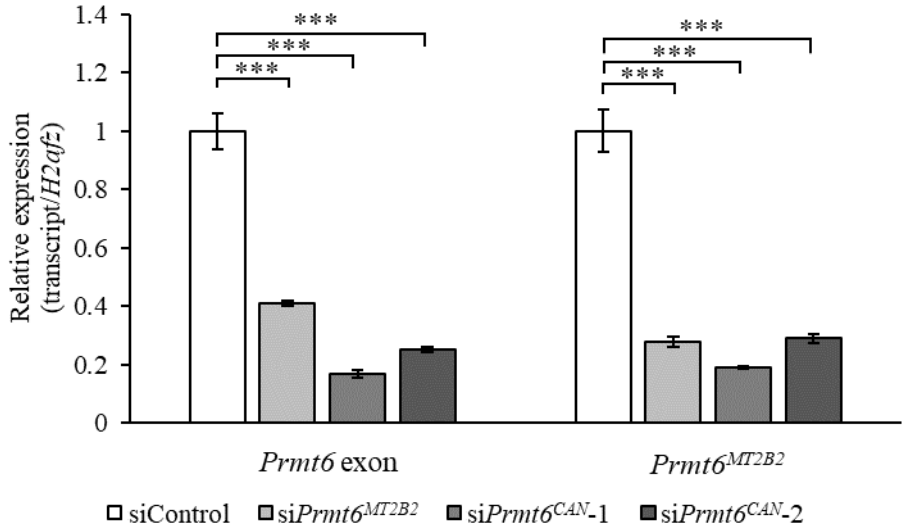

(D) qRT-PCR analysis of *Prmt6* and *Prmt6*^{MT2B2} mRNA abundance in embryos injected with siMT2B2-*Prmt6*, si*Prmt6*-1, si*Prmt6*-2, or siControl in the late two-cell stage. Injection was performed 3–5 h after IVF. The amount of mRNA in siControl-injected embryos was defined as 1, and the expression levels were normalized to *H2afz* as an internal control. Data are expressed as mean ± s.e.m. (n=3). Dunnett's test, ***P < 0.001.

E

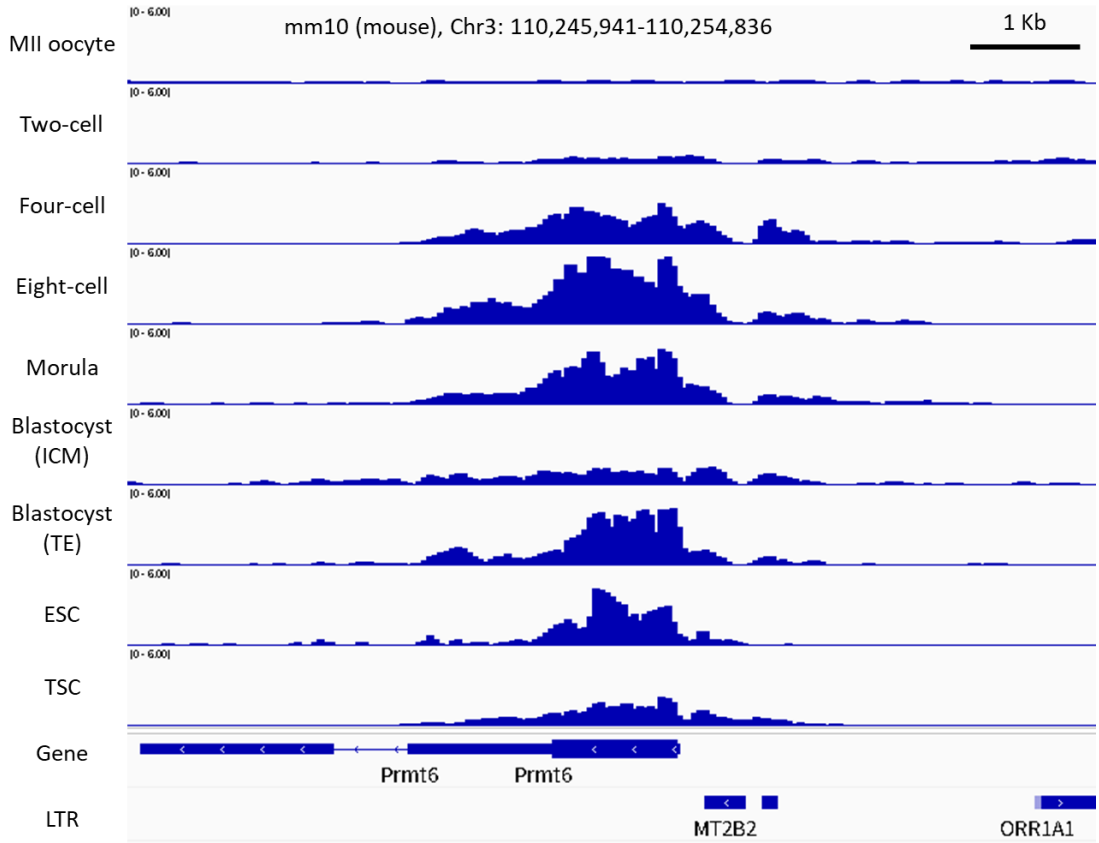

(E) Genome browser view of H3K4me3 ChIP-seq data from each stage of mouse preimplantation embryos. Data for MII oocytes, two-cell embryos, four-cell embryos, eight-cell embryos, morulae, inner cell mass (ICM) and trophectoderm (TE) of blastocysts, embryonic stem cells (ESC), and trophoblast stem cells (TSC) are shown. The *Prmt6*^{CAN} exon and MT2B2 locations are indicated at the bottom.

A

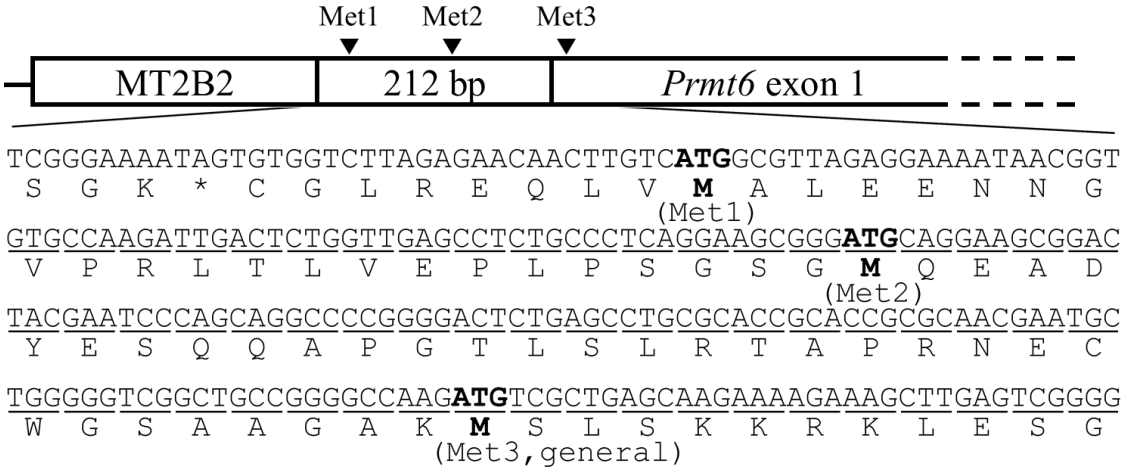

Fig. 3. Protein expression of Prmt6.

(A) Schematic diagram of the genome structure (upper) and genome and protein sequences (lower) of *Prmt6* exon 1. Candidate translation initiation codons (Met1 and Met2) and the canonical translation initiation codon (Met3) are indicated above the schematic diagram and are shown in bold in the sequences.

B

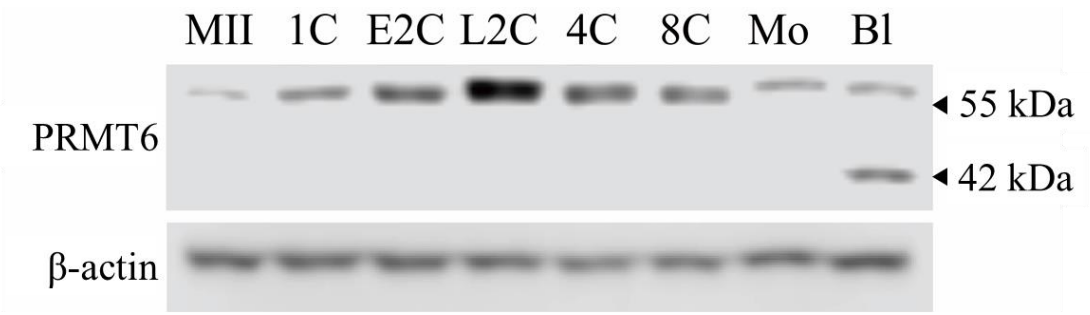

(B) Western blotting of PRMT6 in mouse oocytes and preimplantation embryos. β-actin was used as a loading control. Fifty oocytes or embryos were used in each lane except blastocysts. Twenty-five blastocysts were used. The approximate molecular weight is on the right.

MII: metaphase II oocyte, 1C: one-cell embryo, E2C: early two-cell embryo, L2C: late two-cell embryo, 4C: four-cell embryo, 8C: eight-cell embryo, Mo: morula, Bl: blastocyst

C

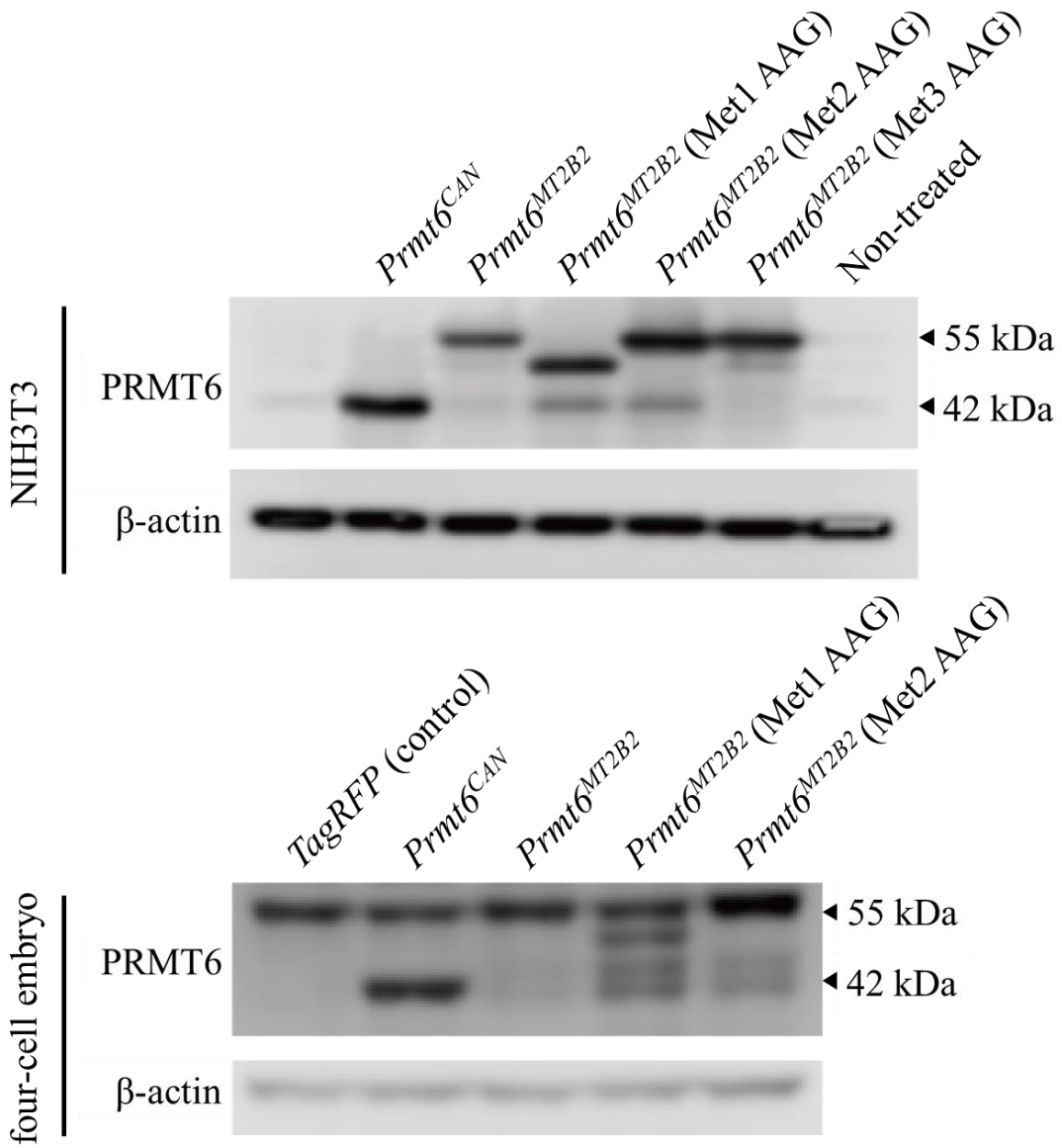

(C) Western blotting analysis for PRMT6 in NIH3T3 cells and four-cell embryos. NIH3T3 cells were transfected with TagRFP mRNA, *Prmt6*^{CAN} mRNA, *Prmt6*^{MT2B2} mRNA, *Prmt6*^{MT2B2} with Met1 mutant mRNA (Met1 AAG), *Prmt6*^{MT2B2} with Met2 mutant mRNA (Met2 AAG), or *Prmt6*^{MT2B2} with Met3 mutant mRNA (Met3 AAG). Zygotes were injected with the same mRNAs except *Prmt6*^{MT2B2} with Met3 mutant mRNA (Met3 AAG) and cultured to the four-cell stage. Fifty embryos were used in

each lane. β-actin was used as a loading control. The approximate molecular weight is on the right.

D

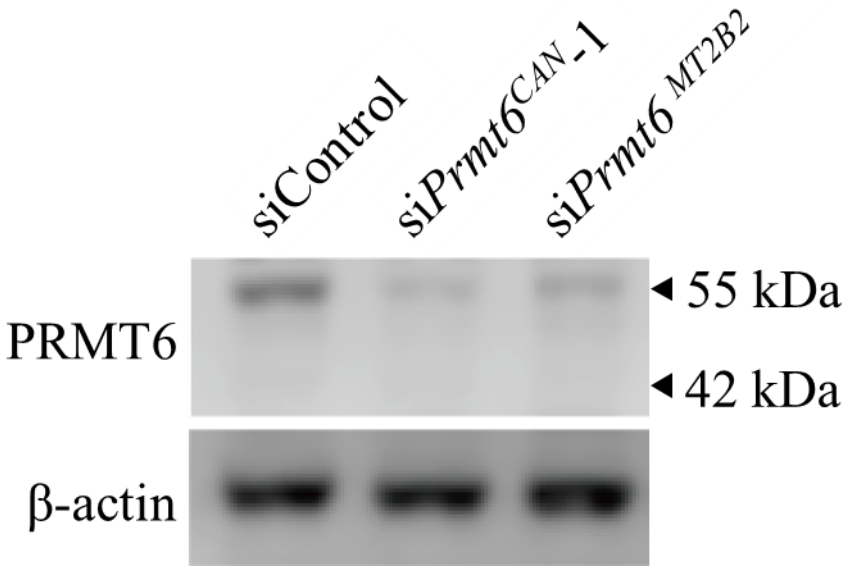

(D) Western blotting analysis of PRMT6 protein in Prmt6-suppressed four-cell embryos. si*Prmt6*^{CAN}-1, si*Prmt6*^{MT2B2}, or siControl was injected into zygote cytoplasm. β-actin was used as a loading control. Fifty embryos were used for each lane. The approximate molecular weight is on the right.

A

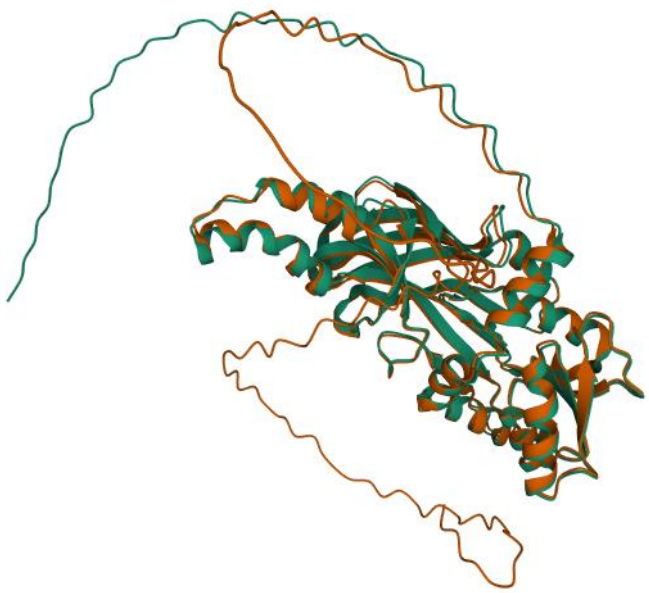

Fig. 4. Substrate-specific histone arginine methylation activity of PRMT6^{MT2B2}.

(A) The 3D structures of PRMT6^{CAN} and PRMT6^{MT2B2} as predicted by AlphaFold2. The green structure represents PRMT6^{CAN} and the orange structure represents PRMT6^{MT2B2}.

B

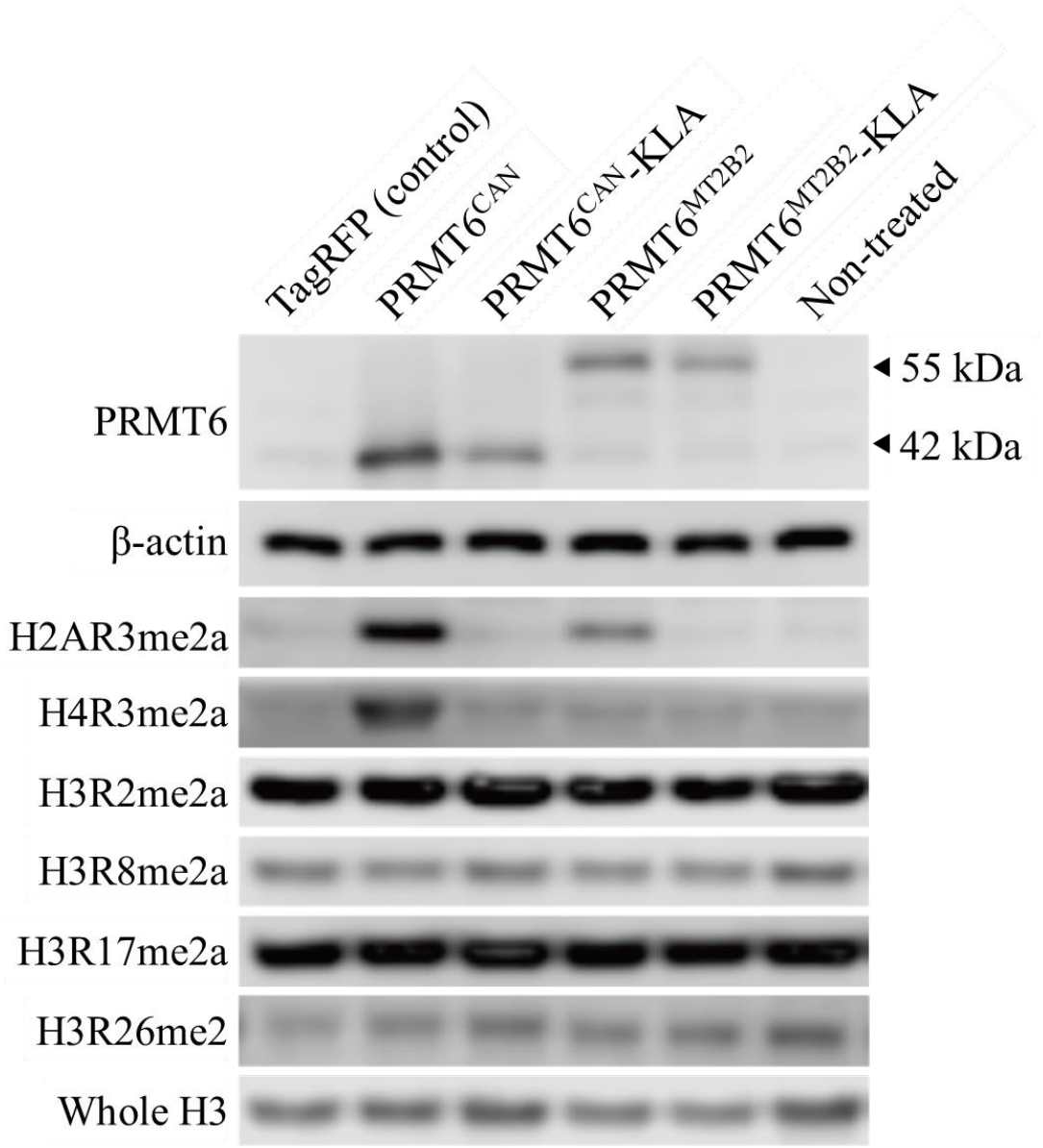

(B) Western blotting analysis of various histone arginine methylation modifications in NIH3T3 cells overexpressing TagRFP, $PRMT6^{CAN}$, $PRMT6^{CAN}$-KLA, $PRMT6^{MT2B2}$, or $PRMT6^{MT2B2}$-KLA. β-actin and whole H3 were used as loading controls. KLA-containing proteins are those in which the enzyme activity is eliminated by replacing amino acids VLD with KLA.

C

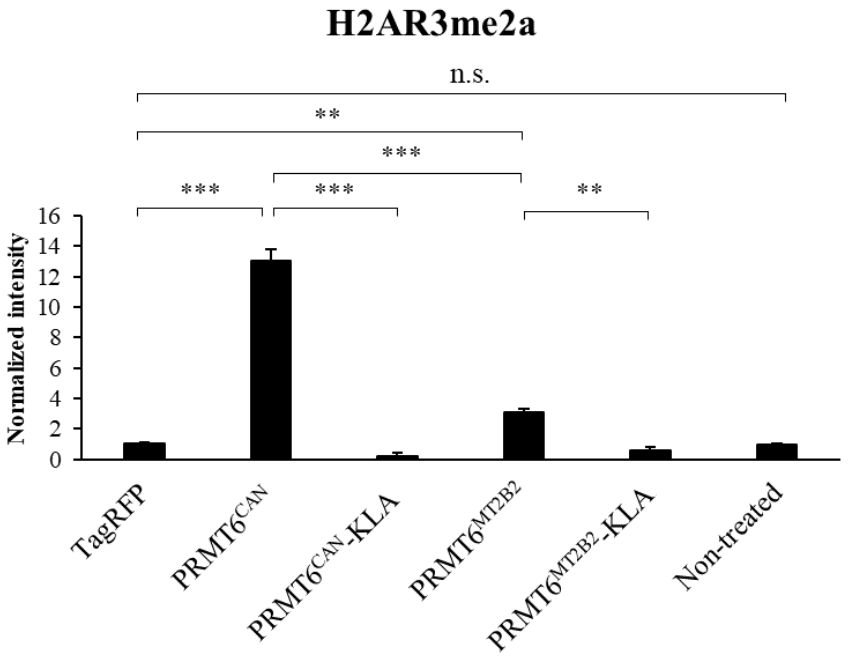
H2AR3me2a
n.s.
**
***
***
***
**
Normalized intensity
16
14
12
10
8
6
4
2
0
TagRFP
PRMT6CAN
PRMT6CAN-KLA
PRMT6MT2B2
PRMT6MT2B2-KLA
Non-treated

D

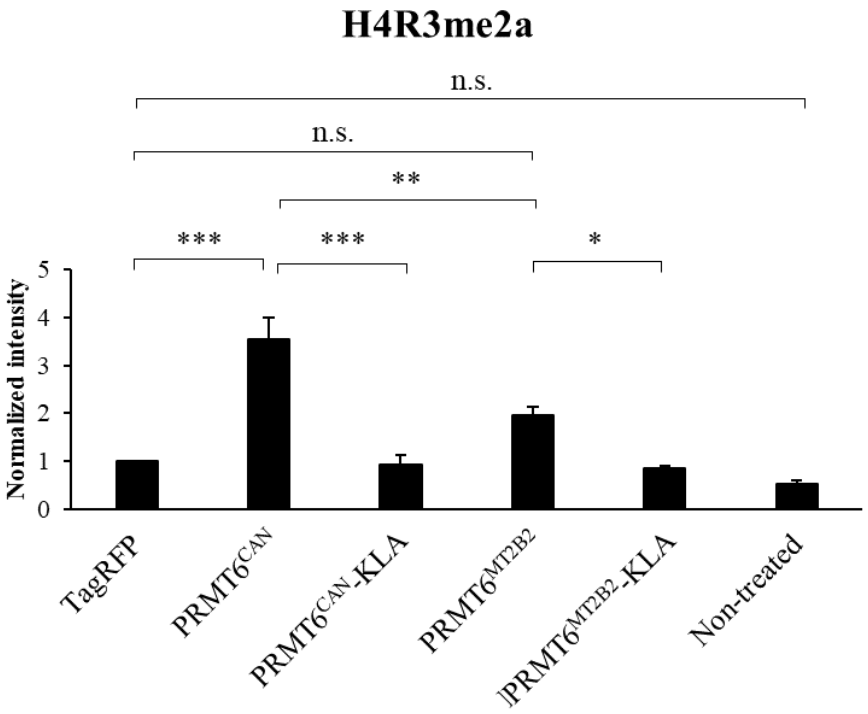
H4R3me2a
n.s.
n.s.
**
***
***
*
Normalized intensity
5
4
3
2
1
0
TagRFP
PRMT6CAN
PRMT6CAN-KLA
PRMT6MT2B2
PRMT6MT2B2-KLA
Non-treated

(C, D) The amounts of H2AR3me2 (C) and H4R3me2 (D) based on the intensity of (B). Overexpression of $PRMT6^{CAN}$ increases H2AR3me2a and H4R3me2a intensity, while overexpression of $PRMT6^{MT2B2}$ increases only H2AR3me2a intensity. Data are expressed as mean ± s.d. (n=3). Tukey-Kramer test, ***$P < 0.001$; **$P < 0.01$; *$P < 0.05$; n.s., not significant.

A

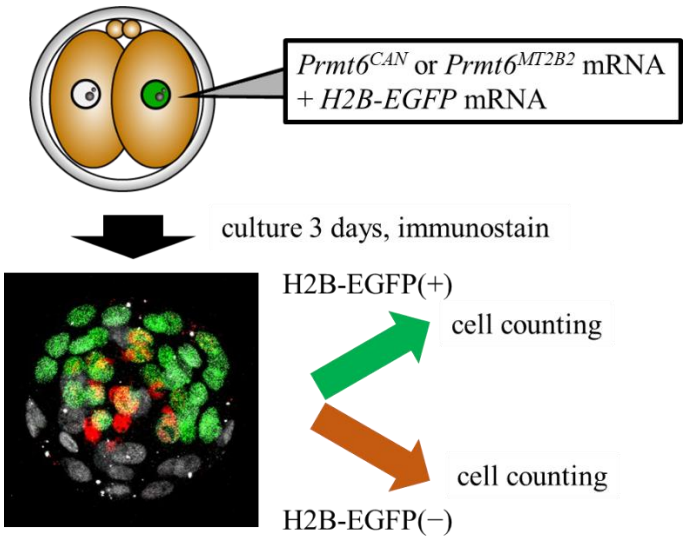

Fig. 5. PRMT6^{MT2B2} determines the cell fate of mouse preimplantation embryos.

(A) Schematic view of the cell fate contribution assay. *Prmt6*^{CAN} or *Prmt6*^{MT2B2} mRNA together with *H2B-EGFP* mRNA was microinjected into one blastomere of two-cell embryos. Embryos cultured until the blastocyst stage (96 hpi) were subjected to immunostaining using antibodies against NANOG (red) and CDX2 (white). Cell nuclei were stained with Hoechst (blue). The number of NANOG-positive cells was counted separately for H2B-EGFP–positive and –negative cells.

B

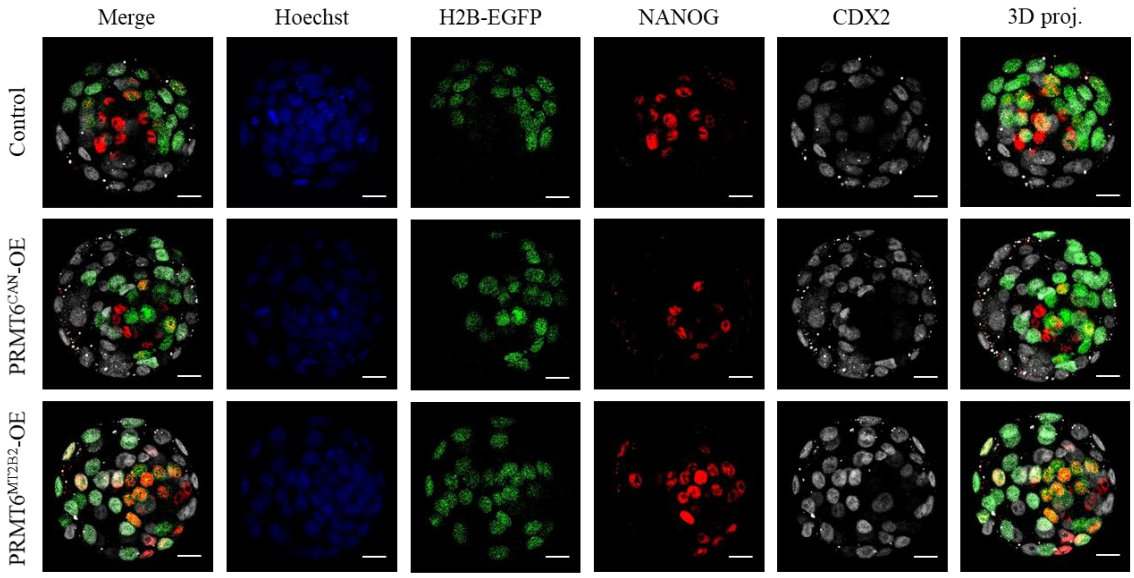

(B) Immunostaining of NANOG and CDX2 in blastocysts overexpressing H2B-EGFP (control), PRMT6^{CAN} with H2B-EGFP (PRMT6^{CAN}-OE), or PRMT6^{MT2B2} with H2B-EGFP (PRMT6^{MT2B2}-OE). Photos are representative of immunostained blastocysts. Hoechst (blue), H2B-EGFP (marker, green), NANOG (red), CDX2 (white), and 3D maximum projections of merged images are shown. Scale bars, 20 μm.

C

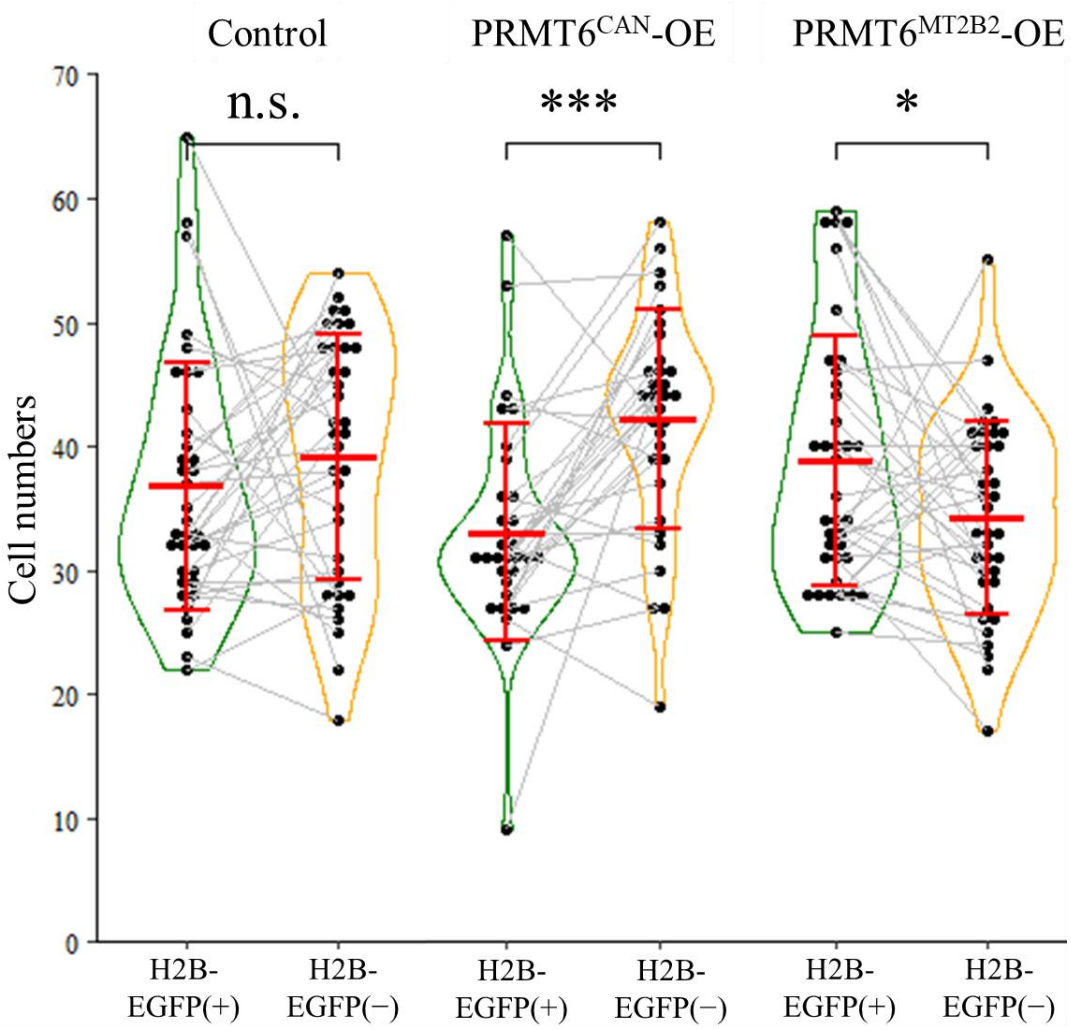

(C) Violin plot depicting the cell numbers of H2B-EGFP–positive (green) or –negative (yellow) cells in control (n=37), PRMT6^{CAN}-OE (n=37), and PRMT6^{MT2B2}-OE (n=32) blastocysts. Each dot represents data from one embryo. The gray lines between dots indicate the same embryos. Red bars and whiskers indicate means and s.d. based on the Wilcoxon signed-rank test, ***$P < 0.001$; *$P < 0.05$; n.s., not significant.

D

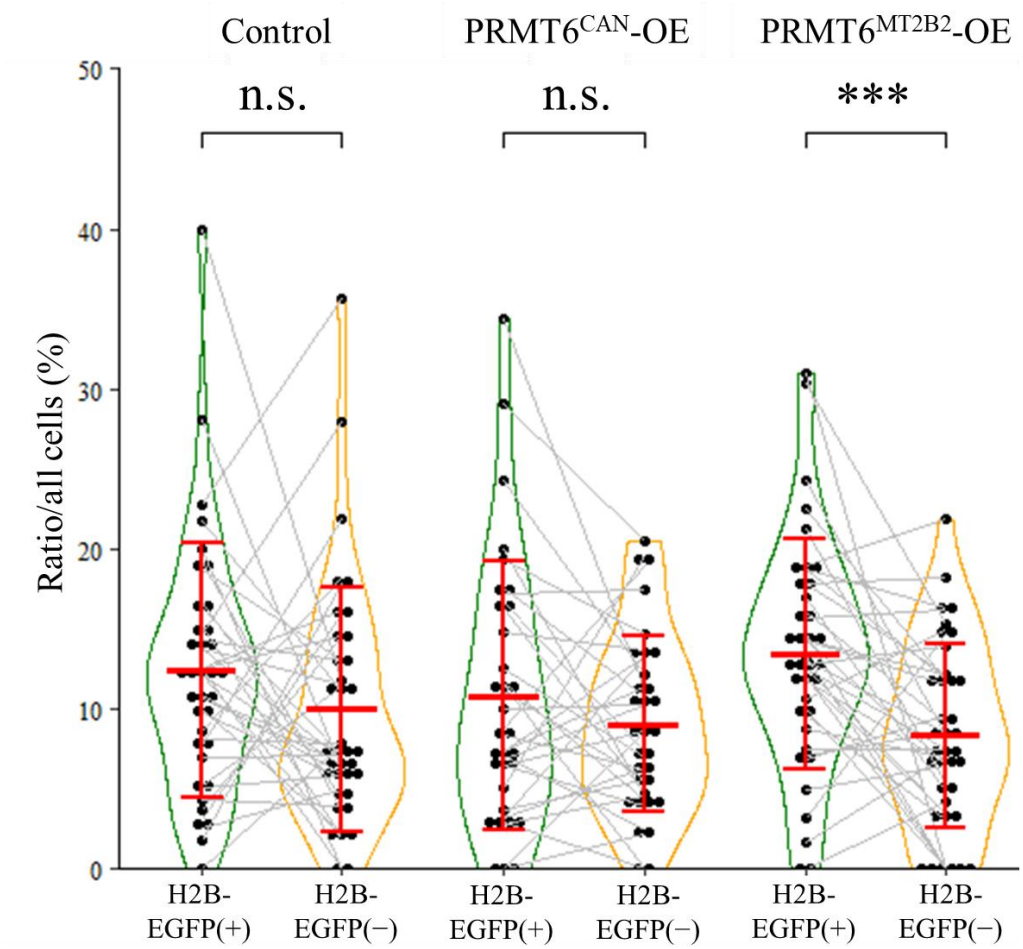

(D) Violin plot depicting the percentage of H2B-GFP–positive (green) or –negative (yellow) cells among cells expressing NANOG in control (n=37), PRMT6^{CAN}-OE (n=37), and PRMT6^{MT2B2}-OE (n=32) blastocysts. Each dot represents data from one embryo. The gray lines between dots indicate the same embryos. The bars and whiskers indicate means and s.d. based on the Wilcoxon signed-rank test, ***$P < 0.001$; n.s., not significant.

Supplementary Data

Supplementary Table 1. Sequences of siRNAs used for microinjection

Names of siRNAs	Sense Strand (5'→3')	Antisense Strand (5'→3')
si*Prmt6* ^{MT2B2}	GCCAAGAUUGACUCUGGUUdTdT	AACCAGAGUCAAUCUUGGCdTdT
si*Prmt6* ^{CAN} -1	GCCGUCUGGUUUCAAGUGAdCdC	UCACUUGAAACCAGACGGCdGdG
si*Prmt6* ^{CAN} -2	CACCGAAGCCUACCGCUUAdGdG	UAAGCGGUAGGCUUCGGUGdCdC
siControl	GUACCGCACGUCAUUCGUAUC	UACGAAUGACGUGCGGUACGU

dT, 2'-deoxythymidine; dC, 2'-deoxycytidine; dG, 2'-deoxyguanosine

Supplementarry Table 2. Primer sequences

for quantitative PCR			
Primer names		Sequences	Product sizes (bp)
Prmt6 exon	sense	AGTGCTACTCCGACGTCTCG	149
	anti-sense	GATGCTGAGAATGCCGGTGC	
Prmt6 ^{MT2B2}	sense	AGGGGTAAAAGGAAAGGGCAA	278
	anti-sense	GTCCCCCGACTCAAGCTTTC	
H2afz	sense	GGTAAAGCGTATCACCCCTCG	130
	anti-sense	CTTCCCGATCAGCGATTTGTG	
for plasmid construction			
Primer names		Sequences	Product sizes (bp)
Prmt6 ^{MT2B2} cloning	sense	AAAGAATTCAGAGAACCCTGACAAGGGGTA	1408
	anti-sense	AAATCTAGATCAGTCCTCCATGGCAAAGTC	
Prmt6 ^{CAN} cloning	sense	AAAGAATTCATGTCGCTGAGCAAGAAAAGAA	1155
	anti-sense	AAATCTAGATCAGTCCTCCATGGCAAAGTC	
Met1 mutation	sense	CTTGTCAAGGCGTTAGAGGAAAATAA	–
	anti-sense	TAACGCCTTGACAAGTTGTTCTCTAA	
Met2 mutation	sense	AGCGGGAAGCAGGAAGCGGACTACGA	–
	anti-sense	TTCCTGCTTCCCGCTTCCTGAGGGCA	
Met3 mutation	sense	GCCAAGAAGTCGCTGAGCAAGAAAAG	–
	anti-sense	CAGCGACTTCTTGGCCCCGGCAGCCG	
KLA mutation	sense	ACGAAGCTTGCGGTGGGCGCGGGCACCGGC	–
	anti-sense	CACCGCAAGCTTCGTCTTGCCTCGCAGCGC	
for in vitro transcription			
Primer names		Sequences	Product sizes (bp)
Prmt6 ^{CAN}, *Prmt6* ^{MT2B2} IVT	sense	TAAGTTGGGTAACGCCAGGG	1351, 1604
	anti-sense	AGCGCGCAATTAACCCTCAC	
H2B-EGFP IVT	sense	TAAGTTGGGTAACGCCAGGG	1501
	anti-sense	GGAGCAGATACGAATGGCTACA	